Phosphodiesterase 2 inhibition preferentially promotes NO/guanylyl cyclase/cGMP signaling to reverse the development of heart failure

Reshma S. Baliga[a,1], Michael E. J. Preedy[a,1], Matthew S. Dukinfield[a], Sandy M. Chu[a], Aisah A. Aubdool[a], Kristen J. Bubb[a], Amie J. Moyes[a], Michael A. Tones[b], and Adrian J. Hobbs[a,2]

[a]William Harvey Research Institute, Barts & The London School of Medicine & Dentistry, Queen Mary University of London, EC1M 6BQ London, United Kingdom; and [b]Pfizer, Inc., St. Louis, MO 63198

Edited by Solomon H. Snyder, Johns Hopkins University School of Medicine, Baltimore, MD, and approved June 26, 2018 (received for review January 18, 2018)

Heart failure (HF) is a shared manifestation of several cardiovascular pathologies, including hypertension and myocardial infarction, and a limited repertoire of treatment modalities entails that the associated morbidity and mortality remain high. Impaired nitric oxide (NO)/guanylyl cyclase (GC)/cyclic guanosine-3′,5′-monophosphate (cGMP) signaling, underpinned, in part, by up-regulation of cyclic nucleotide-hydrolyzing phosphodiesterase (PDE) isozymes, contributes to the pathogenesis of HF, and interventions targeted to enhancing cGMP have proven effective in preclinical models and patients. Numerous PDE isozymes coordinate the regulation of cardiac cGMP in the context of HF; PDE2 expression and activity are up-regulated in experimental and human HF, but a well-defined role for this isoform in pathogenesis has yet to be established, certainly in terms of cGMP signaling. Herein, using a selective pharmacological inhibitor of PDE2, BAY 60-7550, and transgenic mice lacking either NO-sensitive GC-1α (GC-1α$^{-/-}$) or natriuretic peptide-responsive GC-A (GC-A$^{-/-}$), we demonstrate that the blockade of PDE2 promotes cGMP signaling to offset the pathogenesis of experimental HF (induced by pressure overload or sympathetic hyperactivation), reversing the development of left ventricular hypertrophy, compromised contractility, and cardiac fibrosis. Moreover, we show that this beneficial pharmacodynamic profile is maintained in GC-A$^{-/-}$ mice but is absent in animals null for GC-1α or treated with a NO synthase inhibitor, revealing that PDE2 inhibition preferentially enhances NO/GC/cGMP signaling in the setting of HF to exert wide-ranging protection to preserve cardiac structure and function. These data substantiate the targeting of PDE2 in HF as a tangible approach to maximize myocardial cGMP signaling and enhancing therapy.

nitric oxide | natriuretic peptide | cyclic GMP | phosphodiesterase | heart failure

Left ventricular hypertrophy (LVH) and subsequent heart failure (HF) are common to many cardiovascular disorders, including hypertension and myocardial infarction (MI), and, after age, represent the most significant independent risk factors for cardiovascular morbidity and mortality (1). Current therapy focuses on reducing excess fluid load (e.g., diuretics) and blocking neurohormonal pathways (e.g., β-blockers, angiotensin-converting enzyme inhibitors) (2). Unfortunately, these interventions do not offer a cure but only slow deterioration in LV function. Consequently, HF is still associated with a 5-y survival rate of ∼50%; the disorder therefore represents a clear unmet medical need.

Generation of the second-messenger cyclic guanosine-3′,5′-monophosphate (cGMP) by activation of NO-sensitive guanylyl cyclases [$\alpha_1\beta_1$ (GC-1) and $\alpha_2\beta_1$ (GC-2)] (3) and natriuretic peptide-sensitive GCs (GC-A and GC-B) (4) plays a key role in maintaining physiological cardiac contractility and integrity, and in offsetting the pathogenesis of LVH and HF (5). From a homeostatic perspective, endothelial nitric oxide synthase (eNOS) and neuronal NOS (nNOS) appear to function in a complementary manner; eNOS-derived NO is thought to contribute to LV compliance and β-adrenergic inotropy, and to amplify parasympathetic innervation, whereas nNOS-generated NO regulates basal myocardial inotropy and lusitropy via inhibition of the inward calcium current (I_{Ca}), sympathovagal balance, and limitation of the activity of oxidases (6, 7). Indeed, in LVH, such protective NO-mediated systems are depressed, in part, due to diminished NO bioavailability and elevated GC-1/GC-2 heme oxidation (8–10), driven by an increase in the production of reactive oxygen species, particularly by NADPH oxidase isoforms (11). Likewise, natriuretic peptides maintain cardiac structure and function in both physiological and pathological settings, as illustrated by the hypertrophic, fibrotic cardiac phenotype in transgenic animals lacking these mediators or cognate receptors, and the exacerbated response of such mice to cardiac stress (12–14).

From a pharmacological standpoint, NO donors, GC-1/GC-2 [soluble GC (sGC)] stimulators, and exogenously applied natriuretic peptides have been shown to decrease hypertrophy in cardiomyocytes and offset the development of HF in animal models and patients (15, 16). The common generation of cGMP and G-kinase activation affects a plethora of maladaptive, hypertrophic pathways, including functional inhibition of Ca^{2+} channels and Ca^{2+} sequestration (17, 18), calcineurin/nuclear factor of activated T cells (NFAT) signaling (19), blockade of regulators of G protein-signaling (RGS) proteins (20), transient

Significance

The morbidity and mortality associated with heart failure (HF) are unacceptably high. Cyclic guanosine-3′,5′-monophosphate (cGMP) plays a key role in preserving cardiac structure and function, and therapeutically targeting cGMP in HF has shown promise in experimental models and patients. Phosphodiesterases (PDEs) metabolize and curtail the actions of cGMP (and cAMP), and increased PDE activity is thought to contribute to HF pathogenesis. Herein, we show that inhibition of one specific isoform, PDE2, enhances the salutary effects of cGMP in the context of HF, and that this beneficial action facilitates a distinct pathway, driven by nitric oxide, that is impaired in this disorder. These observations validate PDE2 inhibitors as a demonstrable means of boosting cardiac cGMP and advancing HF therapy.

Author contributions: R.S.B., M.E.J.P., M.S.D., S.M.C., A.A.A., K.J.B., A.J.M., M.A.T., and A.J.H. designed research; R.S.B., M.E.J.P., M.S.D., S.M.C., A.A.A., K.J.B., A.J.M., and M.A.T. performed research; M.A.T. contributed new reagents/analytic tools; R.S.B., M.E.J.P., M.S.D., S.M.C., A.A.A., K.J.B., A.J.M., M.A.T., and A.J.H. analyzed data; and R.S.B., M.E.J.P., M.S.D., S.M.C., A.A.A., K.J.B., A.J.M., M.A.T., and A.J.H. wrote the paper.

The authors declare no conflict of interest.

This article is a PNAS Direct Submission.

[1]R.S.B. and M.E.J.P. contributed equally to this work.

[2]To whom correspondence should be addressed. Email: a.j.hobbs@qmul.ac.uk.

This article contains supporting information online at www.pnas.org/lookup/suppl/doi:10.1073/pnas.1800996115/-/DCSupplemental.

Published online July 16, 2018.

receptor potential cation channel (TRPC) (21), and myosin binding protein (MBP)-C (22). This cardioprotective profile of cGMP in HF is exemplified by positive clinical outcomes with the dual neutral endopeptidase (an enzyme that inactivates natriuretic peptides) inhibitor-angiotensin receptor blocker LCZ696 (23) and the sGC stimulator vericiguat (15).

An alternative therapeutic strategy to augment cGMP signaling for cardioprotection is inhibition of phosphodiesterases (PDEs). Cardiac cGMP concentrations are dynamically regulated by GC-driven synthesis in cooperation with degradation mediated by PDEs, a family of enzymes that hydrolyze cGMP and its sibling cyclic adenosine-3′-5′-monophosphate (cAMP) (24). In the heart, PDE isozymes 1, 2, 5, and 9 are believed to exert the most influential effects on cGMP signaling (25–28). Of these, PDE1 is the major isoform expressed in the healthy myocardium (29), whereas PDE5 is only minimally expressed under physiological conditions but significantly up-regulated in the failing myocardium (30, 31). In HF, inhibition of cGMP-metabolizing PDEs 1, 5, and 9 slows pathogenesis (27, 28); indeed, up-regulation of expression and/or activity of PDEs is thought to underpin the diminution of cGMP signaling characteristic of HF (32). Several small clinical studies support a beneficial role for PDE5i in HF (33–36), but the PhosphodiesteRasE-5 Inhibition to Improve CLinical Status And EXercise Capacity in Diastolic Heart Failure (RELAX) trial showed no significant benefit (37). This disappointing outcome intimates that if the therapeutic activity of cGMP is to be harnessed optimally, interventions targeting alternate, or more likely multiple, cGMP synthetic and/or degradative pathways will be necessary.

A relatively unexplored mechanism that might address this therapeutic deficiency is PDE2. This "cGMP-stimulated" PDE metabolizes both cGMP and cAMP, and possesses a GAF-B domain (38) within its N terminus (24) that acts as a negative feedback loop to expedite cyclic nucleotide hydrolysis in the presence of cGMP (akin to PDE5). Three PDE2 splice variants have been identified and are expressed in a wide variety of cells and tissues, including the heart, platelets, and endothelium (24); moreover, PDE2 expression is increased in both animals and patients with HF (39). PDE2 isozymes are kinetically indistinguishable, but the 2A2 and 2A3 variants have an N-terminal membrane localization motif that results in a predominantly particulate distribution. This cellular localization seems to be key to the functioning of PDE2 in the heart due to compartmentalization of cGMP signaling in cardiomyocytes (26, 40), and has been speculated to play a key role in modulating the development of LVH and HF. For example, up-regulation of PDE2 expression and activity may be protective by opposing the effects of sympathetic activation via cAMP breakdown (39, 41, 42). Indeed, PDE2 overexpression has been reported to lower heart rate (HR), maintain LV function and to subdue arrhythmogenesis in experimental MI (43). Alternatively, PDE2 inhibition can prevent the hydrolysis of a localized pool of cAMP, leading to PKA-dependent phosphorylation of NFAT and an antihypertrophic response (44). However, these studies have focused primarily on modulation of cAMP levels (i.e., PDE2 as a "cAMP-hydrolase"), of which chronic, widespread increases are known to cause higher mortality in patients with HF (45). In contrast, there is a paucity of in vivo evidence evaluating the influence of PDE2-mediated cGMP hydrolysis in LVH and HF, although in the setting of pulmonary hypertension (PH), our recent work has highlighted the beneficial effects of PDE2 inhibition in diminishing the vascular remodeling and right ventricular hypertrophy (RVH) (46). Herein, we establish a cGMP-dependent cardioprotective effect of PDE2 in preclinical models of LVH and HF, and identify the GC source of cGMP that drives this process.

Methods

All experiments were conducted according to the Animals (Scientific Procedures) Act of 1986, United Kingdom, and had approval from the QMUL Animal Welfare and Ethical Review Body (AWERB) committee. Animals were housed in a temperature-controlled environment in a 12-h light/dark cycle. Food and water were accessible ad libitum.

Genotyping. Genomic DNA was prepared from ear biopsies for analysis by PCR using standard cycling parameters utilizing the forward and reverse primers listed in *SI Appendix*, Table S1, as we have described previously (47).

Generation of GC-1α Knockout Mice. This GC-1$\alpha^{-/-}$ strain was developed at Pfizer, Inc. Briefly, heterozygous mouse embryonic stem cells containing one GC-1$\alpha^{-/-}$ allele modified by homologous recombination were obtained from Deltagen. Long-distance PCR was used to generate a 5.7-kb 5′ homology arm and a 3.6-kb 3′ homology arm flanking a 5.3-kb deletion encompassing exons 6 and 7 of the mouse GC-1α gene (GenBank accession no. NM_021896). Exons 6 and 7 were replaced with a Lac-Z/Neo^r selection cassette, disrupting the 3′ end of the cyclase domain (*SI Appendix*, Fig. S1). Mouse 129P2/OlaHsd (E14) cells were transformed by established techniques (48), and G418-resistant colonies were selected. Expanded clones were screened via long-distance PCR and Southern blot analysis. One clone with the correctly modified GC-1α allele was used to generate the mouse line via standard blastocyst injection (48).

Successful deletion of GC-1α was confirmed by immunoblot, assay of enzyme activity in lung homogenates, functional vascular pharmacology in response to NO donor, and measurement of mean arterial blood pressure (MABP; *SI Appendix*, Fig. S1). The body weight (BW) of WT and GC-1$\alpha^{-/-}$ mice did not differ significantly at the time of experimentation (WT: 30.92 ± 0.63 g, GC-1$\alpha^{-/-}$: 30.95 ± 0.65 g; $P > 0.05$; $n = 10$).

Expression. Lungs were homogenized in ice-cold 50 mM Tris (pH 7.5), 0.1 mM EDTA, 0.1 mM EGTA, and 0.1% 2-mercaptoethanol containing protease inhibitor mixture (Roche) using an Ultra Turrax T8 disperser (IKA Works, Inc.). Homogenates were centrifuged at 1,000 × *g* for 30 min at 4 °C, the supernatants were collected, and protein concentration was determined using the Bio-Rad method according to the manufacturer's instructions. Twenty micrograms of lung supernatant protein was separated by 7% SDS/PAGE using a Novex Tris-Acetate gel system (Invitrogen), and proteins were transferred to a nitrocellulose membrane (Invitrogen). Staining with Ponceau S Red (Sigma) was used to confirm uniformity of protein loading. Membranes were blocked with 5% milk (Santa Cruz Biotechnology) dissolved in TBS-Tween 20 (pH 7.4; ScyTek Laboratories) for 1.5 h at room temperature. For the detection of GC-1α, membranes were incubated with polyclonal rabbit anti–GC-1α serum (1:2,000 dilution; Alexis Biochemicals), and for the GC-1β subunit detection, they were incubated with polyclonal rabbit anti–GC-1β affinity-isolated antibody (1:1,000 dilution; Alexis Biochemicals) for 1 h at room temperature. Membranes were washed with TBS-Tween 20 (pH 7.4) buffer and incubated with 2° antibody (goat anti-rabbit HRP-conjugated IgG, 1:2,500 dilution; Pierce) for 1 h at room temperature, followed by four washes in TBS-Tween (pH 7.4). Dilutions of primary and secondary antibodies were prepared in TBS-Tween 20 buffer. Antibody reactivity was detected using SuperSignal West Dura Extended Duration Substrate (Thermo Fisher Scientific) and Kodak film (Sigma).

Activity. Assays were performed in 100 μL containing of 50 mM Tris (pH 7.4), 1 mM DTT, 0.2 mM GTP, 5 mM $MgCl_2$, 0.5 mM 3-isobutyl-1-methylxanthine, and 1–10 μg of lung extract protein. The NO donor DETA-NONOate (DETA; 100 μM) was included as specified. Reactions were started by addition of substrate, incubated for 60 min at 37 °C, and terminated with the addition of 20 mM EDTA. cGMP was then quantified using a CatchPoint cGMP Fluorescent Assay Kit (Molecular Devices) according to the manufacturer's instructions.

Vascular reactivity. The vascular reactivity of mouse thoracic aortic vascular ring preparations was determined using classical tissue bath pharmacology, as we have described previously (49).

Blood pressure and HR. Blood pressure was recorded in conscious freely moving mice using radiotelemetric transmitters (TA11PA-C10; Data Sciences International) implanted into the aortic arch, as we have described previously (49).

Pressure Overload-Induced HF. Pressure overload LVH and cardiac dysfunction were induced by performing abdominal aortic constriction (AAC) at the suprarenal level. Male WT, GC-1$\alpha^{-/-}$ (as described above), and GC-A$^{-/-}$ (kind gift of O. Smithies, University of North Carolina at Chapel Hill, Chapel Hill, NC) mice (21–23 g; offspring of heterozygote parents to enable use of corresponding WT littermate controls) were anesthetized (1.5% isoflurane in O_2), body temperature was maintained at 37 °C, and the analgesic buprenorphine (0.1 mg/kg) was administered (i.m.). An incision was made in the abdominal cavity, and the abdominal aorta was separated from the surrounding tissue at the suprarenal level. Aortic constriction was performed by tying a 4-0 surgical thread against a 25-gauge needle between the superior mesenteric and renal arteries. This produces a 30% constriction of the luminal diameter (50). For sham operations, the 4-0 surgical thread was passed under the aorta and removed without tying it against the needle. In some studies, WT mice undergoing AAC were administered the NOS inhibitor L-N^G-nitroarginine

PHARMACOLOGY

methylester (L-NAME; 100 mg·kg^{-1}·d^{-1}) via the drinking water for 7 d before and during the AAC model.

Chronic Sympathetic Activation-Induced HF. Sustained sympathetic activation is characteristic of HF and can be recapitulated in preclinical models using chronic dosing with the β-agonist isoproterenol (ISO) (51). Male WT, GC-1α$^{-/-}$, and GC-A$^{-/-}$ mice (24–25 g) were infused s.c. with ISO (20 mg·kg^{-1}·d^{-1} for 14 d; Sigma–Aldrich) via osmotic minipumps (model 1002; Alzet). Saline containing 0.5% ascorbic acid was used as the solvent for ISO to avoid catecholamine oxidation over time.

Treatment Regimens. Animals were assigned randomly to receive the selective PDE2 inhibitor BAY 60-7550 (52) (10 mg·kg^{-1}·d^{-1}; kind gift of J.-P. Stasch and P. Sandner, Bayer AG, Wuppertal, Germany) or vehicle control (0.5% carboxycellulose + 10% polyethylene glycol) by daily oral gavage, initiated 3 wk after AAC or 1 wk after ISO infusion (i.e., after the HF phenotype had developed).

In Vivo Cardiac Functional Assessments. In vivo cardiac morphology and function were assessed by M-mode echocardiography using a VisualSonics Vevo 770 echocardiographic system and a 30-MHz transducer. Mice were anesthetized (1.5% isoflurane in O_2), and body temperature was maintained at 37 °C. LV internal diameter (LVID) and LV posterior wall thicknesses at diastole (d) and systole (s) were measured from short-axis M-mode images. LV ejection fraction (EF%) was calculated as follows: LVEF% = $[(\text{LVIDd})^3 - (\text{LVIDs})^3]/(\text{LVIDd})^3 \times 100$; LV fractional shortening (FS%) was calculated as follows: LVFS % = (LVIDd − LVIDs)/LVIDd × 100. Values were averaged from three beats.

Langendorff Isolated Heart Preparations. Ex vivo cardiac function and the effects of acute PDE2 inhibition were evaluated in murine hearts set up in Langendorff mode, as we have described previously (53). Acute changes in these parameters were recorded in response to bolus injections of ANP (0.01–10 nmol), the NO donor sodium nitroprusside (SNP; 0.01–10 nmol), the endothelium-dependent vasodilator acetylcholine (0.1–1.0 nmol), and the β-agonist ISO (1–100 pmol) in the absence and presence of BAY 60-7550 (100 nM).

Histology Staining and Imaging. The isolated left ventricles were cut transversely below the mitral valves, fixed in 10% formalin for 24 h, and then stored in 70% alcohol before embedding in paraffin wax and sectioning.

Wheat Germ Agglutinin Fluorescence Staining. Ventricular myocyte size was determined by staining heart sections with a fluorescent cell membrane antibody, wheat germ agglutinin (WGA) Alexa Fluor 647 (Molecular Probes, Invitrogen), and mounted with Prolong gold DAPI mountant as per standard immunohistochemistry protocols. Images were taken on a Zeiss 710 confocal microscope, and the cardiomyocyte size was analyzed with ImageJ (NIH). The cardiomyocyte size was estimated by an investigator blinded to treatment type and as an average of ∼400 cells per heart.

Picrosirius Red Staining. Tissue slides were dewaxed, rehydrated and stained using a Picrosirius Red Stain Kit following the manufacturer's instructions (Polysciences, Inc.). A Nikon Eclipse TS100 microscope (Nikon UK Limited) was used to capture images of the stained slides. Images were analyzed by threshold analysis using ImageJ, with the investigator blinded to treatment type.

Primary Cardiomyocyte Isolation and Culturing. Primary cardiomyocytes were isolated using a Pierce Primary Cardiomyocyte Isolation Kit (Thermo Fisher Scientific) with minor modifications. Briefly, individual neonatal hearts from 1- to 3-d-old mice were minced and treated with cardiomyocyte isolation enzyme 1 (with papain) and cardiomyocyte isolation enzyme 2 (with thermolysin). The resulting isolated cardiomyocytes were seeded into gelatin (0.1%)-precoated 12-well plates and incubated in DMEM for 3 d until confluent. The cells were then serum starved for 24 h before treatment with angiotensin II (Ang II; 1 μM) for 24 h in the absence and presence of DETA (10 μM), atrial natriuretic peptide (ANP; 1 μM), or brain natriuretic peptide (BNP; 1 μM) under basal conditions or following treatment with BAY 60-7550 (100 nM). Light microscopy images of beating cardiomyocytes were taken at 0 h (baseline) and 24 h. ImageJ was used to analyze the cardiomyocyte size. Averages of 30 cells per heart and six hearts per treatment were analyzed.

Quantitative RT-PCR, Immunoblotting, and Immunohistochemistry. Whole hearts were homogenized using QIAshredder technology (Qiagen), and RNA was extracted using a standard extraction kit (Qiagen). RNA was quantified using a NanoDrop spectrophotometer (Thermo Fisher Scientific), and 1 μg was converted to cDNA by reverse transcription (High Capacity RNA-to-cDNA Kit; Applied Biosystems, Life Technologies Ltd). Specific primers for PDE2A (54), hypertrophic or fibrotic markers, and housekeeping genes RLP-19 and β-actin (300 nM; detailed in *SI Appendix*, Table S2) were added to cDNA template and SyBr Green quantitative PCR mix (Quantitect SYBR Green Kit; Qiagen). Twenty nanograms of cDNA from each sample was amplified using quantitative real-time PCR over 40 cycles (initial denaturation: 10 min at 95 °C; cycling: 45 cycles for 10 s at 95 °C, 15 s at 57 °C, and 5 s at 72 °C; melt: 68–90 °C). mRNA expression was analyzed by expressing the cycle threshold (Ct) value as $2^{-\Delta\Delta Ct}$ and normalized to both housekeeping genes (RPL-19 and β-actin).

PDE2A protein expression was determined by immunoblot using primary anti-PDE2A antibody (1:500; Santa Cruz Biotechnology) and secondary horseradish peroxidase-conjugated anti-goat IgG antibody (1:10,000; Santa Cruz Biotechnology). Bands were quantitated by densitometry using ImageJ and normalized to the loading control, anti-GAPDH (1:50,000; Thermo Fisher Scientific), and secondary antibody horseradish peroxidase-conjugated anti-mouse IgG (1:5,000; Dako).

PDE2A localization was assessed in heart sections by employing conjugated WGA (Alexa Fluor 647; Molecular Probes, Invitrogen) staining to outline cardiomyocyte boundaries. Slides were then double stained with anti-PDE2A antibody (as above; Santa Cruz Biotechnology) and mounted with Prolong Gold DAPI mountant as per standard immunohistochemistry protocols. All slides were imaged using a Hamamatsu nanozoomer S60 (40× magnification).

Terminal deoxynucleotidyl transferase-mediated dUTP nick end labeling (TUNEL) staining was conducted to assess levels of apoptosis in heart sections using a commercially available kit (MK500; Takara Bio, Inc.). All slides were imaged using a Hamamatsu nanozoomer S60 (20× magnification). TUNEL-positive cells and DAPI-stained nuclei were manually counted by quantitative image analysis using ImageJ. A positive control consisting of paraffin-embedded sections of rat mammary gland was supplied as part of the kit.

PDE2 Activity. PDE2 activity in whole-heart homogenates was determined by assaying the concentration of cGMP and cAMP in the absence and presence of BAY 60-7550 (10 mg·kg^{-1}·d^{-1}) in vivo using commercially available kits (Direct cGMP and Direct cAMP; Enzo Life Sciences).

Data Analysis. Results are expressed as mean ± SEM, and $P < 0.05$ denotes significance. The *n* value denotes the number of animals used in each group, and data were analyzed (GraphPad Prism, version 5; GraphPad) using one-way or two-way ANOVA with a Bonferroni post hoc test as appropriate.

Results

PDE2 Inhibition Reverses Experimental HF in Response to Pressure Overload. AAC brought about a sustained increase in MABP (*SI Appendix*, Table S3) and an archetypal HF phenotype as expected, comprising reduced contractility, LVH, and LV dilatation (Fig. 1). Cardiomyocyte size and Picrosirius Red staining were also increased, indicative of a hypertrophied and fibrotic left ventricle (Fig. 1 and *SI Appendix*, Fig. S2). Administration of BAY 60-7550 at week 3 resulted in a significant reversal of each of these indices of disease severity (Fig. 1 and *SI Appendix*, Fig. S1); indeed, in some cases, the salutary effect of PDE2 inhibition was so pronounced that structure (e.g., cardiomyocyte size) and function (e.g., EF) were ostensibly returned to normal levels (Fig. 1). Importantly, administration of BAY 60-7550 did not cause a significant reduction in MABP (*SI Appendix*, Table S3), excluding the possibility that PDE2 inhibition may lead to peripheral dilatation and a reduction in the cardiac overload, thereby indirectly dampening the HF phenotype, and BAY 60-7550 did not overtly alter HR (*SI Appendix*, Table S4). These findings verify a substantial, multifaceted protective effect of PDE2 inhibition in HF.

The Beneficial Effects of PDE2 Inhibition in Pressure Overload-Induced HF Are Not Underpinned by Acute Changes in Cardiac Function. One potential mechanism by which PDE2 inhibition might bring about a beneficial effect in the setting of HF, in terms of myocardial function, would be to exert an acute, positive inotropic effect, thereby augmenting contractility. To rule this out, hearts from sham animals and mice undergoing AAC were isolated and set up in Langendorff mode to assess the effects of BAY 60-7550 per se, as well as on the actions of cGMP (i.e., NO, natriuretic peptides)- and cAMP (ISO)-elevating agents. Cardiac structure and function were recorded longitudinally by echocardiography to ensure an HF phenotype was established in the mice undergoing AAC, and

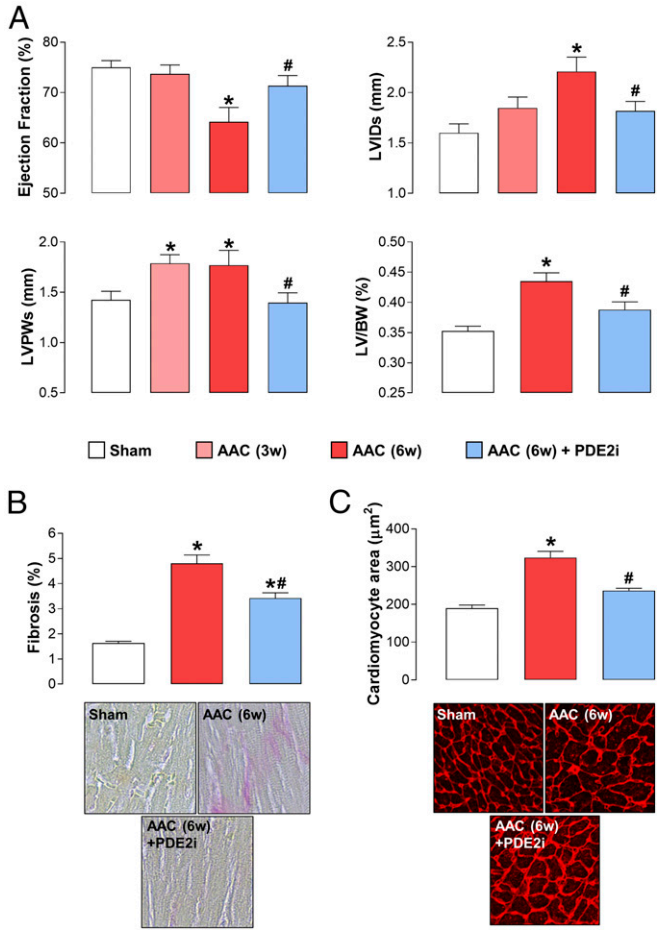

Fig. 1. PDE2 inhibition reverses experimental HF in response to pressure overload. Echocardiographic indices of heart structure and function (*A*), cardiac fibrosis (Magnification: 40×.) (*B*), and cardiomyocyte size (Magnification: 20×.) (*C*) are shown in sham mice and animals undergoing AAC for 3 wk (3w) or 6 wk (6w) in the absence and presence of BAY 60-7550 (10 mg·kg^{-1}·d^{-1} p.o., initiated at 3w). Data are expressed as mean ± SEM and analyzed by one-way ANOVA with a Bonferroni post hoc test. *$P < 0.05$ versus sham; $^{\#}P < 0.05$ versus AAC (6w) (n = 12–18).

this was corroborated by initial data from the hearts ex vivo, which exhibited reduced contractility and impaired coronary function (*SI Appendix*, Fig. S3). BAY 60-7550 caused a modest, yet significant, fall in coronary perfusion pressure (CPP) in isolated hearts indicative of a subtle vasodilator effect (Fig. 2). This vasorelaxant activity was present regardless of whether the hearts were isolated from sham animals or mice with HF. Addition of ANP caused a dose-dependent reduction in CPP but had little or no effect on contractility (i.e., LVDP) or HR (Fig. 2). These responses were not affected by the presence of BAY 60-7550 or in failing hearts. Bolus delivery of SNP also caused a dose-dependent fall in CPP, was devoid of activity against LVDP, but tended to increase HR (Fig. 2). Again, this profile was maintained in sham and failing hearts, and in the absence and presence of BAY 60-7550, with the only exception being a reduction in vasodilation in response to PDE2 inhibition in hearts from animals with AAC (Fig. 2). Finally, ISO caused a dose-dependent drop in CPP with a concomitant, overt increase in LVDP and HR, as anticipated for a cAMP-elevating agent. This coronary vasodilator activity and positive inotropic and chronotropic action were equivalent in sham and failing hearts and in the presence of BAY 60-7550 (apart from a slight reduction in coronary vasodilator activity with PDE2 inhibition in failing hearts; Fig. 2). BAY 60-7550 was unable to augment the positive inotropic and chronotropic actions of ISO in this setting, establishing that metabolism of the pool of cAMP that regulates contractility and rate in sham or failing hearts is not a key role for PDE2; this dovetails well with a lack of effect of BAY 60-7550 on HR in vivo (*SI Appendix*, Table S4). These data clearly demonstrate that the favorable effects of BAY 60-7550 are not underpinned by an acute action on cardiac contractility but, instead, are exerted via a more extensive, chronic influence on heart morphology [and potentially additional mechanisms, including autonomic regulation (55, 56)].

PDE2 Inhibition Reverses Pressure Overload-Induced HF in GC-A$^{-/-}$ Mice. We next sought to determine which arm of the GC enzyme family was responsible for generating the pool of cGMP regulated by PDE2. Since our previous work in PH had highlighted a link between PDE2 and natriuretic peptide/GC-A–dependent cGMP synthesis, and due to the fact that genetic deletion of ANP, BNP, or GC-A results in cardiac structural and functional deficits at baseline (12–14), we investigated the efficacy of BAY 60-7550 in pressure overload-induced HF in GC-A$^{-/-}$ mice. Unexpectedly, the beneficial effects of PDE2 inhibition on cardiac structure and function in AAC-driven HF in WT mice were maintained in GC-A$^{-/-}$ animals (Fig. 3). As published

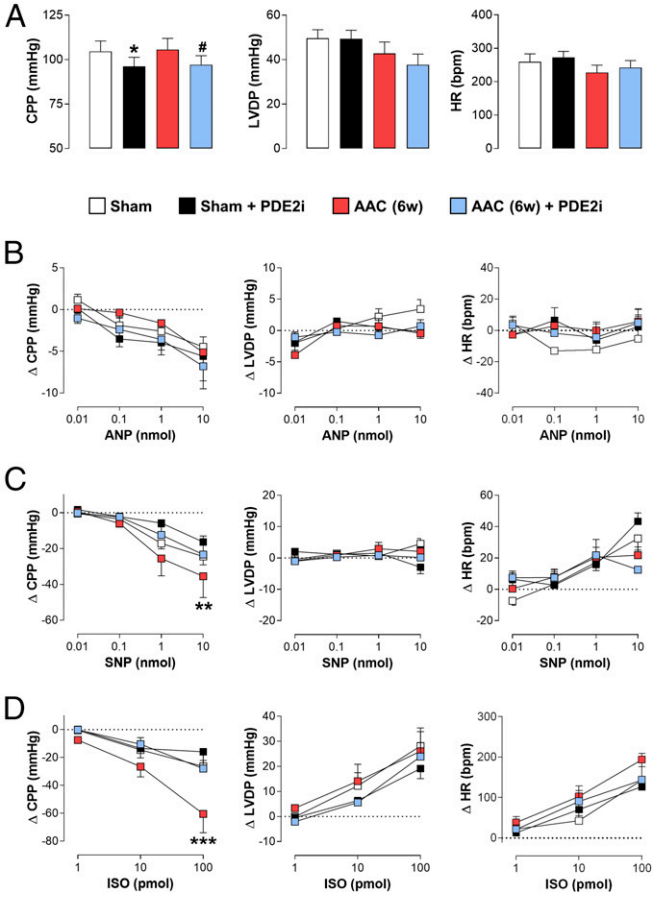

Fig. 2. Beneficial effect of PDE2 inhibition in pressure overload-induced HF is not underpinned by acute changes in cardiac function. (*A*) CPP, LV developed pressure (LVDP), and HR in WT sham mice or animals subjected to 6 wk (6w) of ACC in the absence and presence of acute administration of BAY 60-7550 (100 nM). CPP, LVDP, and HR are shown in sham mice and animals subjected to 6w of AAC in the absence and presence of BAY 60-7550 (10 mg·kg^{-1}·d^{-1} p.o., initiated at 3w) following the addition of increasing doses of ANP (*B*), SNP (*C*), and ISO (*D*). Data are expressed as mean ± SEM and analyzed by one-way ANOVA with a Bonferroni post hoc test (*A*) or two-way ANOVA (*B*–*D*). *$P <$ 0.01 versus sham, $^{\#}P < 0.05$ versus AAC (6w; *A*); **$P < 0.01$, ***$P < 0.001$ versus AAC+ PDE2i (6w; *C* and *D*) (n = 6–12).

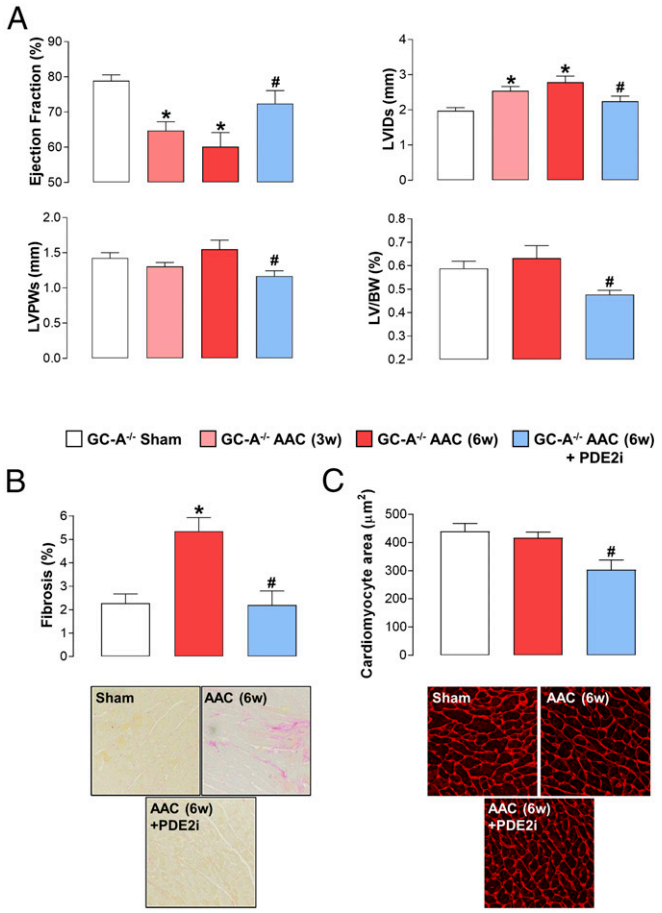

Fig. 3. PDE2 inhibition reverses pressure overload-induced HF in GC-A$^{-/-}$ mice. Echocardiographic indices of heart structure and function (*A*), cardiac fibrosis (Magnification: 40×.) (*B*), and cardiomyocyte size (Magnification: 20×.) (*C*) are shown in sham mice and animals undergoing AAC for 3 wk (3w) or 6 wk (6w) in the absence and presence of BAY 60-7550 (10 mg·kg^{-1}·d^{-1} p.o., initiated at 3w) are shown. Data are expressed as mean ± SEM and analyzed by one-way ANOVA with a Bonferroni post hoc test. *$P < 0.05$ versus sham; $^{\#}P < 0.05$ versus AAC (6w) (n = 6–12).

previously, the GC-A$^{-/-}$ animals had marked intrinsic cardiac hypertrophy and dilatation (albeit with preserved EF; Fig. 3). Nonetheless, the reduction in contractility, increase in ventricular wall thickness and mass, and fibrotic burden were all significantly reversed in the presence of BAY 60-7550 (Fig. 3); PDE2i also caused a reduction in cardiomyocyte size. Indeed, the positive pharmacodynamic profile of BAY 60-7550 was of a magnitude similar to that observed in WT mice (Fig. 1). Such findings argue against a significant contribution of ANP/BNP signaling to the salutary actions of PDE2i in HF.

Obligatory Role of NO/GC-1α Signaling in the Beneficial Effects of PDE2 Inhibition. As a result of the preserved pharmacology of BAY 60-7550 in GC-A$^{-/-}$ mice, we turned to exploration of a potential role for the NO/GC-1/cGMP pathway. We took two approaches: first, using a transgenic strain with global deletion of the GC-1α subunit (GC-1α$^{-/-}$) and, second, treating WT animals with the NOS inhibitor L-NAME. The cardiovascular phenotype of the GC-1α$^{-/-}$ strain generated herein mirrored that reported previously (57, 58), with loss of GC-1α protein, reduced vasorelaxant and cGMP-generating capacity of NO donors, and sex-dependent hypertension (*SI Appendix*, Fig. S1).

GC-1α$^{-/-}$ mice exhibited a subtle cardiac phenotype at baseline, with a modest rise in LVID and increased cardiomyocyte size (albeit without a significant increase in the LV/BW ratio in comparison to WT mice) (Fig. 4). In response to AAC, GC-1α$^{-/-}$ animals exhibited an almost identical phenotype to WT mice, with reduced cardiac contractility, enlarged and dilated left ventricles, and an increase in fibrosis. Of note, the baseline cardiomyocyte size in GC-1α$^{-/-}$ mice was increased compared with WT animals; consequently, AAC only marginally increased this index of hypertrophy (Fig. 4). The mechanism underpinning this innate cardiomyocyte enlargement, but normal LV mass, in GC-1α$^{-/-}$ animals is not a result of cardiomyocyte loss since levels of apoptosis were not different from those in WT mice (*SI Appendix*, Fig. S4); the reason for this intrinsic difference remains to be explained. Regardless, in sharp contrast to WT and GC-A$^{-/-}$ mice, PDE2i did little or nothing to improve the cardiac function in GC-1α$^{-/-}$ animals (Fig. 4). To substantiate this critical involvement of NO/GC-1/cGMP signaling in the salutary effects of PDE2i, essentially identical studies were conducted in WT mice receiving L-NAME (*SI Appendix*, Fig. S5). First, the consequences of pan-NOS inhibition per se on cardiac function following AAC were minimal, reflecting the phenotype of GC-1α$^{-/-}$ animals. Second, mirroring observations in GC-1α$^{-/-}$ mice, the pharmacodynamic benefit of BAY 60-7550 was completely absent, including effects to reverse the fibrotic burden that had been maintained in GC-1α$^{-/-}$ animals (*SI Appendix*, Fig. S5). Notably, GC-1α expression tended to be upregulated in response to pressure overload (*SI Appendix*, Fig. S2).

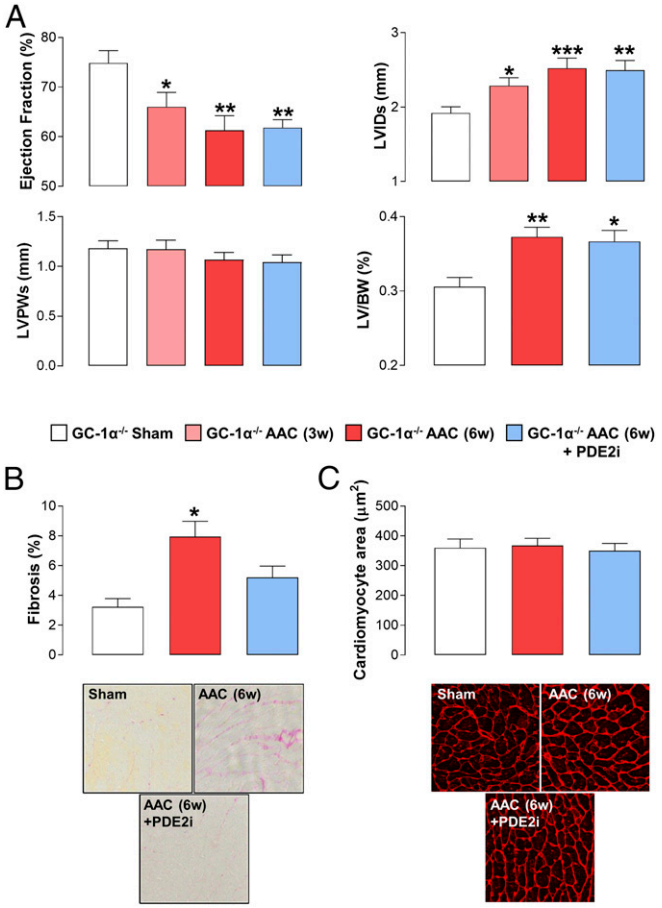

Fig. 4. Obligatory role of GC-1/NO signaling in the beneficial effects of PDE2 inhibition in HF. Echocardiographic indices of heart structure and function (*A*), cardiac fibrosis (Magnification: 40×.) (*B*), and cardiomyocyte size (Magnification: 20×.) (*C*) are shown in sham mice and animals undergoing AAC for 3 wk (3w) or 6 wk (6w) in the absence and presence of BAY 60-7550 (10 mg·kg^{-1}·d^{-1} p.o., initiated at 3w). Data are expressed as mean ± SEM and analyzed by one-way ANOVA with a Bonferroni post hoc test. *$P < 0.05$ versus sham; **$P < 0.01$ versus sham; ***$P < 0.001$ versus sham (n = 6–12).

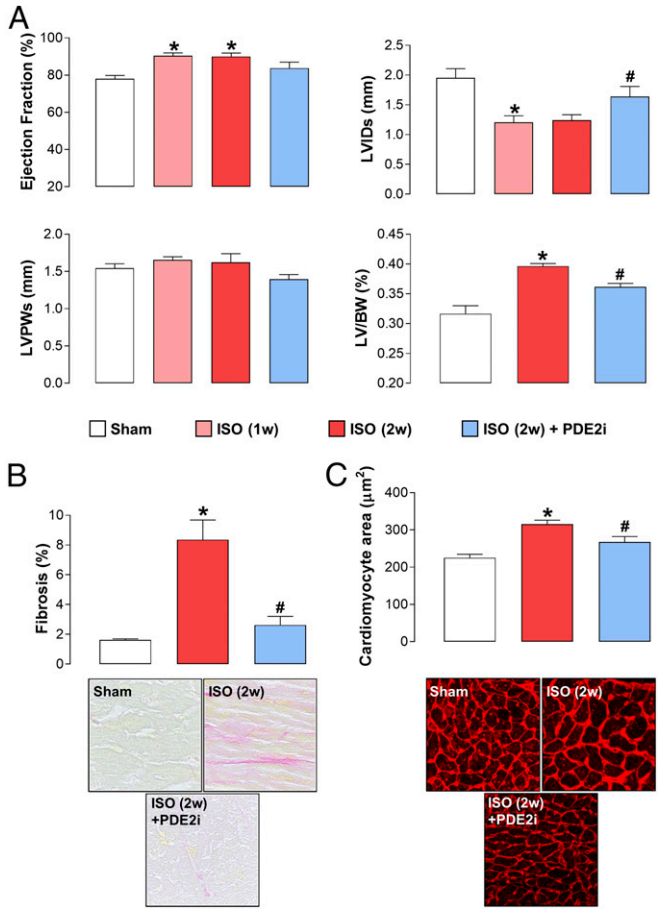

Fig. 5. PDE2 inhibition reverses experimental HF in response to sympathetic hyperactivation. Echocardiographic indices of heart structure and function (*A*), cardiac fibrosis (Magnification: 40×.) (*B*), and cardiomyocyte size (Magnification: 20×.) (*C*) are shown in sham mice and animals administered ISO (20 mg·kg^{-1}·d^{-1} s.c.) for 2 wk (2w) in the absence and presence of BAY 60-7550 [10 mg·kg^{-1}·d^{-1} p.o., initiated at 1 wk (1w)]. Data are expressed as mean ± SEM and analyzed by one-way ANOVA with a Bonferroni post hoc test. *P < 0.05 versus sham; $^{\#}P$ < 0.05 versus AAC (6 wk) (n = 6–12).

These data provide genetic and pharmacological verification that it is the NO-driven arm of cGMP signaling that is responsible for the positive effects of PDE2i in HF.

PDE2 Inhibition Reverses Experimental HF in Response to Sympathetic Hyperactivation in a NO/GC-1α–Dependent, but GC-A–Independent, Manner. To demonstrate that PDE2 inhibition has a generic salutary effect in experimental models of HF, the efficacy of BAY 60-7550 was also explored in ISO-driven (i.e., sympathetic hyperactivation) cardiac dysfunction. Akin to pressure overload, PDE2i brought about a multimodal protection to reverse the cardiac contractile changes (in this instance, more analogous to HFpEF), LV hypertrophy and dilatation, and cardiac fibrosis (Fig. 5). Furthermore, substantiating the concept that PDE2i augments NO/GC-1α signaling in HF, the positive outcome realized by BAY 60-7550 was maintained in GC-A$^{-/-}$ mice (Fig. 6) but diminished or lost in GC-1α$^{-/-}$ animals (Fig. 7). Interestingly, genetic deletion of GC-A transformed the predominantly HFpEF phenotype produced by ISO to HFrHF, with a severely impaired EF resulting in death in many animals (Fig. 6), confirming the critical role(s) of endogenous natriuretic peptide signaling in preserving cardiac function in HF (14). However, BAY 60-7550 was still able to reverse this pathology and significantly improve mortality (Fig. 6), proffering further evidence that targeting NO/GC-1 signaling is pharmacologically beneficial in HF, a thesis strengthened by the lack of efficacy of BAY 60-7550 in GC-1α$^{-/-}$ mice exposed to ISO (Fig. 7). A global comparison of the cardiac structural and functional indices in pressure overload-induced HF in WT, GC-A$^{-/-}$, and GC-1α$^{-/-}$ mice is depicted in *SI Appendix*, Fig. S6.

This model, characterized by excessive β-adrenoreceptor/cAMP signaling, also served as a means to tease out any cAMP-driven effects of PDE2 inhibition. In this regard, however, BAY 60-7550 did not exert any positive chronotropic effects (*SI Appendix*, Table S4).

PDE2 Inhibition Boosts the Antihypertrophic Effect of NO, but Not Natriuretic Peptides, in Isolated Cardiomyocytes. To corroborate the importance of NO/GC-1/cGMP signaling to the HF phenotype, we followed up in vivo investigations with in vitro studies in isolated cardiomyocytes. Here, addition of NO, ANP, and BNP reduced the hypertrophic response (i.e., cardiomyocyte area) to Ang II (Fig. 8). Notably, however, the reduced hypertrophic response to NO, but not ANP or BNP, significantly increased in the presence of BAY 60-7550 (Fig. 8). This in vitro model of cardiomyocyte hypertrophy presents further evidence of the compartmentalization of NO/GC-1/cGMP signaling with PDE2 in murine hearts.

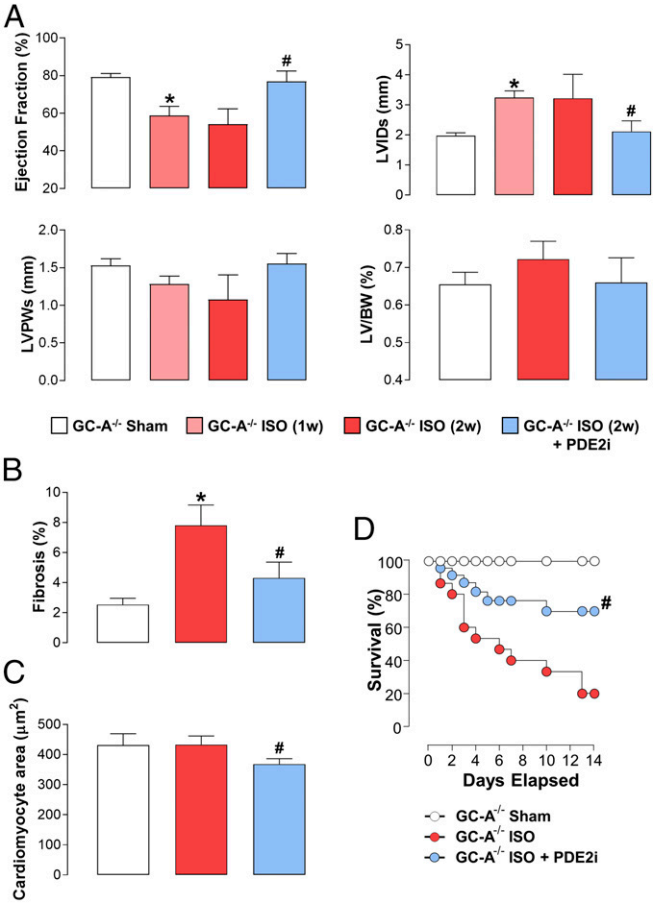

Fig. 6. PDE2 inhibition reverses sympathetic hyperactivation-induced HF in GC-A$^{-/-}$ mice. Echocardiographic indices of heart structure and function (*A*), cardiac fibrosis (*B*), and cardiomyocyte size (*C*) are shown in sham mice and animals administered ISO (20 mg·kg^{-1}·d^{-1} s.c.) for 2 wk (2w) in the absence and presence of BAY 60-7550 [10 mg·kg^{-1}·d^{-1} p.o., initiated at 1 wk (1w)]. (*D*) Survival in sham mice and animals administered ISO (20 mg·kg^{-1}·d^{-1} s.c.) for 2w in the absence and presence of BAY 60-7550 (10 mg·kg^{-1}·d^{-1} p.o., initiated at day 0). Data are expressed as mean ± SEM and analyzed by one-way ANOVA with a Bonferroni post hoc test (*A*–*C*) or as a Kaplan–Meier survival plot (*D*). *P < 0.05 versus sham; $^{\#}P$ < 0.05 versus AAC (6 wk; *A*–*C*) or GC-A$^{-/-}$ + ISO (*D*) (n = 6–12).

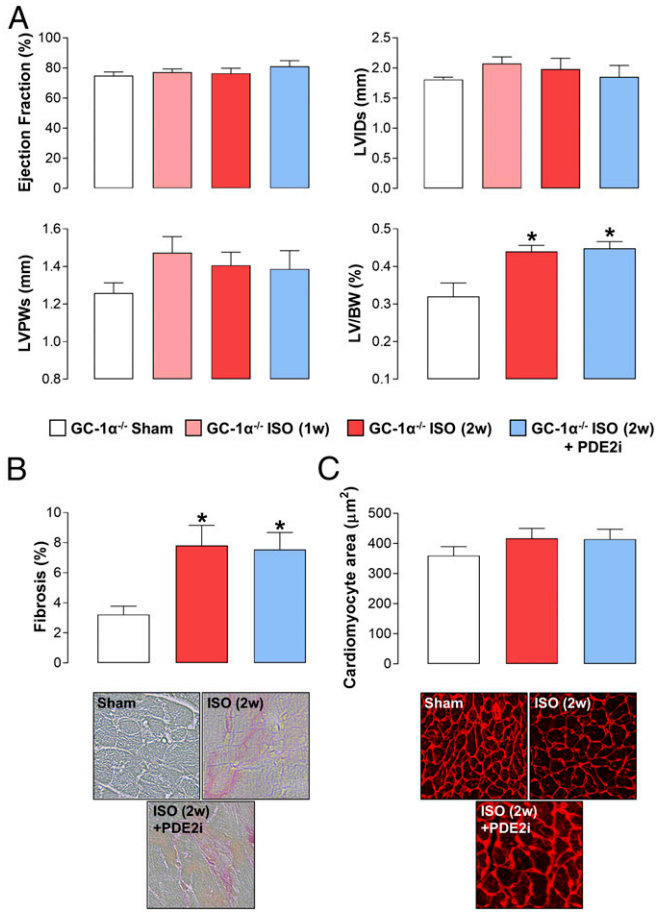

Fig. 7. Obligatory role of GC-1/NO signaling in the beneficial effects of PDE2 inhibition in sympathetic hyperactivation-induced HF. Echocardiographic indices of heart structure and function (*A*), cardiac fibrosis (Magnification: 40×.) (*B*), and cardiomyocyte size (Magnification: 20×.) (*C*) are shown in sham mice and animals administered ISO (20 mg·kg^{-1}·d^{-1} s.c.) for 2 wk (2w) in the absence and presence of BAY 60-7550 [10 mg·kg^{-1}·d^{-1} p.o., initiated at 1 wk (1w)]. Data are expressed as mean ± SEM and analyzed by one-way ANOVA with a Bonferroni post hoc test. *$P < 0.05$ versus sham ($n = 6$–12).

PDE2 Inhibition Augments Cardiac cGMP, but Not cAMP, Levels. To explore the cGMP- and cAMP-hydrolyzing activity of PDE2 in healthy and failing hearts, cardiac cyclic nucleotide concentrations were determined in the in vivo models. AAC increased cGMP levels modestly (~50%) in WT animals, but these values were markedly enhanced (~300%) following ACC in the presence of BAY 60-7550 (Fig. 8), indicating that PDE2 activity is markedly up-regulated in HF and plays a central role in curbing cGMP signaling. This pattern of activity was entirely absent in GC-1α$^{-/-}$ hearts but maintained in GC-A$^{-/-}$ hearts (Fig. 8), paralleling the in vivo functional pharmacology. In contrast, BAY 60-7550 was unable to influence global cAMP levels in WT animals with AAC (Fig. 8), which fits with previous reports of the compartmentalized effects of PDE2 inhibition on local pools of cAMP (40) (which would entail a lack of effect on overall cardiac cAMP concentrations); alternatively, PDE2 may not play a key role in cAMP metabolism in this setting.

Finally, the expression of PDE2A was up-regulated in hearts from mice undergoing AAC (Fig. 8), consistent with published data in animal models and patients with HF (39); however, this recognized increase in PDE2A was not as pronounced in the sympathetic hyperactivation model (*SI Appendix*, Fig. S2), despite the clear pharmacological benefit of PDE2i; this suggests the trigger(s) for promoting PDE2A expression is specific to pressure overload rather than enhanced sympathetic drive. In addition, PDE2A appeared to exhibit somewhat of a sarcomeric localization (i.e., a striated staining pattern), but this did not change patently in the face of pressure overload, implying that PDE2A localization does not spatially adjust during HF to physically associate with a different cGMP pool (*SI Appendix*, Fig. S7).

PDE2 Inhibition Reduces the Expression and/or Activity of a Number of Prohypertrophic and Profibrotic Signaling Pathways. To glean molecular insight into the downstream pathways coupled to NO/GC-1α signaling in the context of PDE2i in HF, we employed quantitative PCR to interrogate a number of established cardiac hypertrophic and fibrotic mediators (59). Here, administration of BAY 60-7550 resulted in reduced expression of a number of profibrotic markers (e.g., Col1α1, Col1α2) and drivers (e.g., TGF-β, CTGF), albeit without affecting ColIVα1 or fibronectin (*SI Appendix*, Fig. S8); this profile matched the strong antifibrotic effect observed in vivo. The antihypertrophic action of PDE2i documented in vivo was supported by a significant reduction in ANP and β-MHC expression, but this did not appear to occur via

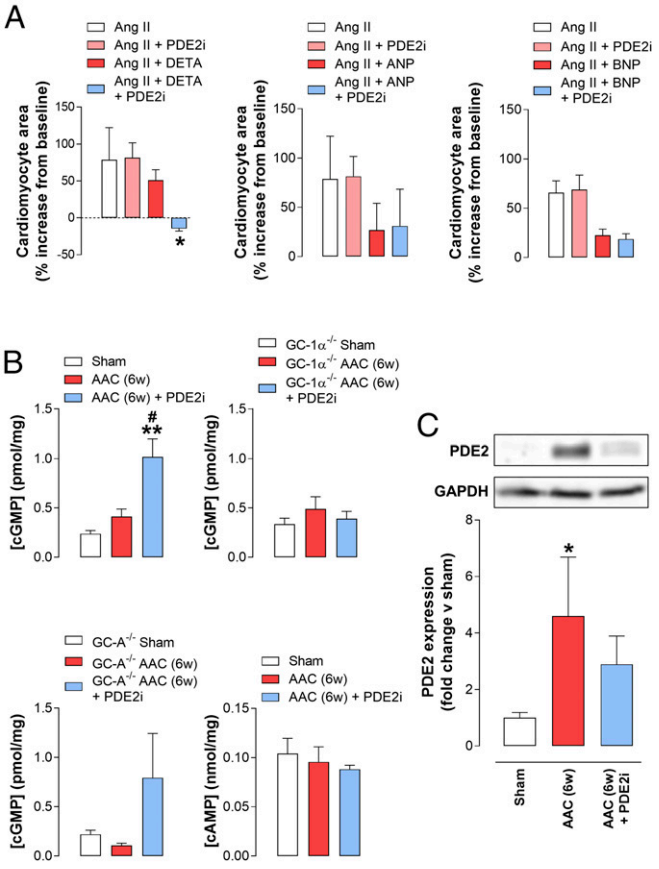

Fig. 8. PDE2 inhibition augments cardiac cGMP, but not cAMP, levels in vivo and promotes the antihypertrophic effect of NO, but not ANP, in isolated cardiomyocytes. (*A*) Cardiomyocyte area in cells isolated from neonatal WT mice treated with Ang II (100 nM) for 24 h in the absence and presence of the NO donor DETA (10 μM), ANP (1 μM), or BNP (1 μM) under basal conditions or following treatment with BAY 60-7550 (100 nM). (*B*) Cyclic nucleotide levels in whole-heart homogenates from sham mice or animals subjected to AAC for 6 wk (6w) in the absence and presence of BAY 60-7550 (10 mg·kg^{-1}·d^{-1} p.o., initiated at 3 wk). (*C*) Immunoblot analysis of PDE2A expression in whole-heart homogenates from mice subjected to AAC for 6w in the absence and presence of BAY 60-7550 (10 mg·kg^{-1}·d^{-1} p.o., initiated at 3 wk). Data are expressed as mean ± SEM with analysis by one-way ANOVA with a Bonferroni post hoc test. *$P < 0.05$ versus Ang II + DETA (*A*); **$P < 0.01$ versus sham versus ACC, $^{\#}P < 0.05$ versus AAC (*B*); *$P < 0.05$ versus sham (*C*) ($n = 6$).

significant modulation of established prohypertrophic pathways, such as NFAT or GSK3β (*SI Appendix*, Fig. S8).

Discussion

The strategy of promoting cardiac cGMP signaling, by dual neutral endopeptidase/angiotensin receptor blockers or sGC stimulators, is clinically effective in HF (15, 23). Blockade of several PDE isoforms, including PDE1 (25), PDE5 (27), or PDE9 (28), has shown promise in experimental models of HF, suggesting that targeting these cGMP-hydrolyzing enzymes may also offer therapeutic gain, although a large-scale clinical evaluation of PDE5 inhibition in patients with HFpEF did not meet its primary end point (37). Previous work has demonstrated positive pharmacology through inhibition of an additional PDE isozyme, PDE2, in restoring pulmonary hemodynamics, vascular remodeling, and RVH in preclinical models of PH (46). Increased expression and activity of PDE2 in experimental models (60, 61) and patients with HF (39) provide support for also targeting this isozyme in HF; however, previous studies have largely focused on the cAMP-hydrolyzing capacity of the enzyme, with both positive (44) and negative (39) outcomes. The present study took a functional approach to evaluate the capacity of PDE2 as a cGMP-hydrolyzing enzyme to modulate the pathogenesis of experimental HF. Using both pressure overload and ISO-induced LVH and cardiac dysfunction, we describe that PDE2 expression and activity are up-regulated as a consequence of disease, and that PDE2 inhibition proffers a multipronged protective effect. In both models, the decline in contractility, LVH, LV dilatation, and fibrotic lesions was halted, and often reversed, by administration of the selective PDE2i BAY 60-7550. This was mirrored, at a more molecular level, by increases in cardiac cGMP (but not cAMP) levels and diminution of a range of hypertrophic and fibrotic markers. These observations suggest PDE2 plays a central role in the reduced cGMP signaling that has been shown to characterize HF, at least in experimental models, leading to misaligned myocardial energetics, compromised cardiac performance, and coronary vascular dysfunction (62). Moreover, inhibition of this PDE isozyme may represent a novel means by which to promote cardiac cGMP signaling for therapeutic gain.

To determine if the beneficial effects of PDE2 inhibition in experimental HF were dependent on cGMP derived from NO- or natriuretic peptide-sensitive GCs, we conducted parallel studies in animals deficient in either cGMP-dependent signaling system. In this setting, the positive effect of BAY 60-7550 on cardiac dysfunction was maintained in GC-A$^{-/-}$ mice [the cognate receptor for ANP and BNP (63)] but was absent in animals harboring a genetic deletion of GC-1α. In a logical extension to these findings, studies were repeated in animals treated chronically with the nonselective NOS inhibitor L-NAME; an identical response profile was observed in that the efficacy of BAY 60-7550 apparent in WT mice was completely abrogated. This finding indicates that the up-regulation of PDE2 curtails, specifically, NO/GC-1/cGMP signal transduction to exert a cardioprotective benefit in HF, but does little or nothing to alter natriuretic peptide-triggered pathways that are well established to be antihypertrophic and antifibrotic (13, 14, 63). Indeed, this differential mechanism of action is illustrated perfectly in the sympathetic hyperactivation model, where genetic deletion of GC-A$^{-/-}$ resulted in significant mortality (i.e., an inherent cardioprotective function of ANP/BNP) but rescued by administration of BAY 60-7550 (i.e., augmenting NO/GC-1 signaling). These data suggest that PDE2 inhibitors may be an effective means by which to promote cardioprotective NO/GC-1/cGMP signaling and offset the deterioration in LV function typical of patients with HF.

These data align well with the observation that PDE2 can be allosterically activated by NO/GC-1–derived cGMP to modulate cAMP bioactivity in cardiac myocytes (40). However, in terms of functional cGMP effects, cell-based studies have intimated that membrane-bound PDE2 is more efficient in hydrolyzing particulate GC-generated cGMP as a result of intracellular compartmentalization (26). Nevertheless, the colocalization of GC-1 with chaperones that promote association with the cytoplasmic membrane [e.g., Hsp70 (64), Hsp90 (65)] does provide the rationale for a local pool of GC-1–generated cGMP in close proximity to PDE2. This concept is supported by nNOS translocation to the plasma membrane in failing hearts (66) and by the fact that caveolin binding protects GC-1 from translocation, oxidation, and loss of NO sensitivity in response to volume overload (8, 67). A similar pattern of activity was observed in terms of changes in coronary flow in isolated hearts. Here, BAY 60-7550 caused a modest vasodilatation in hearts from WT and GC-A$^{-/-}$ mice, but this effect was absent in hearts lacking GC-1α; again, this suggests PDE2 blockade enhances signaling by (endothelium-derived) NO/GC-1 in the coronary vasculature. This dilator effect on coronary function, albeit modest, would be a welcome additional action of PDE2 inhibitors in the context of HF since it would promote increased blood flow to the myocardium. Interestingly, however, PDE2 inhibition did not augment SNP-induced vasodilatation in the coronary circulation, suggesting it might exert a subtle effect on endothelium-derived NO bioactivity rather than on agonist-stimulated dilatation. Despite the pharmacological benefit of PDE2 inhibition and augmentation of NO/GC-1/cGMP signaling in HF models in WT mice, we noted that genetic deletion of GC-1α did not cause a significant intrinsic deterioration in the cardiac dysfunction associated with AAC. This fits with previous work reporting that eNOS$^{-/-}$, GC-1α$^{-/-}$, and cardiomyocyte-specific G-kinase (cGK) I$^{-/-}$ mice do not exhibit exacerbated LVH in response to pressure overload in the context of hypertension (58, 68) and/or AAC (50, 69) [although more stringent thoracic aortic constriction does tease out an aggravated phenotype (70, 71)]. The reason for this apparent disconnect is almost certainly the release of natriuretic peptides upon cardiac stress, which is sufficient to maintain relatively intact cardiac structure and function (68). This observation therefore suggests that NO/GC-1/cGMP signaling does not innately impact the development of LVH and HF, but can be harnessed pharmacologically to provide a therapeutic benefit. This is despite the fact that GC-1α expression tends to be up-regulated in response to pressure overload. The logical explanation for this is that impairment of this signaling cascade, for example, through eNOS uncoupling (10), GC-1β heme oxidation (8, 67), and/or up-regulation of PDEs (25, 27, 28), diminishes its influence to such an extent that only under circumstances of pharmacological augmentation can it meaningfully affect disease progression. The downstream signaling pathways driven by PDE2-regulated cGMP pools to bring about this beneficial action on NO/GC-1 signaling warrant further investigation. Involvement of cGKI in the antihypertrophic and antifibrotic actions of cGMP does not always appear to be a prerequisite (69, 72–74), but the kinase is known to modify well-established targets, including Ca^{2+} channels and Ca^{2+} sequestration (17, 18), calcineurin/NFAT signaling (19), RGS (20), TRPC6 (21), and MBP-C (22). Activation of cGKII might represent an alternate pathway since this cGK isoform in tandem with PDE2 is responsible for governing aldosterone production in the adrenal cortex (75). Reports that PDE2 regulates the cGMP-dependent sympatholytic effects of NO (and natriuretic peptides) (55, 56) also proffer an intriguing mechanism that might underlie the benefits of PDE2 inhibition in HF.

One explanation for the beneficial effects of PDE2 inhibition on the HF phenotype could be an acute positive inotropic effect via augmentation of cAMP signaling (since this PDE isozyme metabolizes both cGMP and cAMP), which would tend to functionally oppose the failing myocardium. This phenomenon has been reported previously in mice using BAY 60-7550 or animals overexpressing a cardiac-specific PDE2 (43). To test this possibility, isolated hearts from WT, GC-1α$^{-/-}$, and GC-A$^{-/-}$ mice that had undergone pressure-overload or sham surgery were set up in Langendorff mode. While the lack of sympathetic innervation represents a patent caveat in this setting, it enables examination of more acute responses in the myocardium and coronary vasculature, with sympathetic stimulation being mimicked by administration of ISO. In hearts removed from animals exposed

to AAC, myocardial contractility and coronary vascular function were both impaired compared with hearts from sham-operated animals, commensurate with an HF phenotype. Importantly, while BAY 60-7550 had a small effect on increasing coronary flow in both normal and failing hearts, it was unable to alter any inotropic or chronotropic effects of NO donors, ANP, or ISO. Also, there was no observable change in HR in the presence of BAY 60-7550 (as an index of cardiac cAMP functionality) in either pressure overload- or ISO-induced HF. In concert, these observations suggest that PDE2 inhibition has little or no acute effect on cardiac function, even in the face of β-receptor stimulation, and that the beneficial effects we report in experimental HF in vivo are therefore longer term actions on heart structure and the hypertrophic/fibrotic response. Curiously, these observations seem to be at odds with recent data describing positive chronotropic effects of BAY 60-7550 in mice with acute or chronic β-adrenoreceptor activation (43); whether the lower in vivo dose in the present study (10 $mg{\cdot}kg^{-1}{\cdot}d^{-1}$ p.o. versus 3 mg/kg bolus i.p.) explains the lack of effect on cAMP signaling remains to be established (even if that is the case, it means a tenable window of opportunity exists permitting differentiation between cGMP and cAMP, if required). Conversely, a parallel approach employing transgenic mice overexpressing cardiac-specific PDE2 revealed a significant increase in LV mass at baseline and following MI (43), which would dovetail well with a cardioprotective role for PDE2 underpinned by cGMP.

Recent work has revealed that PDE2 changes its substrate profile in the left ventricle based on the dynamic levels of cGMP and cAMP. Thus, under physiological circumstances, PDE2 hydrolyses cGMP almost exclusively, whereas in the presence of β-adrenergic activation, PDE2 predominantly metabolizes cAMP, thereby restricting adrenergic signaling (26, 40, 61). Our data suggest that PDE2, in experimental models of HF in vivo and in isolated hearts ex vivo, acts primarily as a "cGMP-hydrolase"; however, although we only provide a cursory inspection herein, PDE2A localization does not appear to change overtly in response to pressure overload. However, this does not rule out an effect of PDE2i on a local pool of cAMP that promotes antihypertrophic activity, as has been recently reported (44); one shortcoming of the present study is that such a confined change would not have been detectable in the whole-heart cyclic nucleotide analysis. Indeed, it would be advantageous to target PDE2 in HF if the enzyme regulated generic antihypertrophic mechanisms involving both cyclic nucleotides (without an overt effect on contraction/metabolic demand). Interestingly, however, these observations are in contrast to contemporary reports describing cross-talk between CNP-triggered cGMP accumulation and cAMP-driven increases in contractility at the level of PDE3 in HF (76). Further investigation is required to determine if the cGMP-elevating activity of PDE2i might indirectly inhibit PDE3 in a similar fashion; again, our assessment of global cyclic nucleotide levels would likely have missed such a compartmentalized effect; however, from a functional perspective (i.e., inotropy), this did not seem to be an issue. Additionally, utilization of GC-$A^{-/-}$ mice would not have brought to light an effect on CNP signaling in this context since this natriuretic peptide triggers cGMP generation via GC-B.

The differential activity of NO/GC-1 and natriuretic peptide/GC-A signaling has important implications for the pharmacological manipulation of cGMP for cardioprotective purposes in HF. Ultimately, it seems likely that multiple interventions, targeted at both the NO- and natriuretic peptide-dependent GC/cGMP systems, will provide the optimal pharmacological boost since while there is overlap in the two pathways (e.g., antihypertrophic, vasodilator), there are clearly distinct consequences (e.g., antiplatelet versus natriuretic). Thus, it is important that the compartmentalized nature of cGMP (and cAMP) signaling be further delineated, with the aim of identifying the most efficient interventions that can achieve this therapeutic goal. Whether this might be inhibiting multiple PDEs; blocking breakdown with concomitant cyclase activation; or, most likely, parallel activation of NO- and natriuretic peptide-signaling pathways remains to be verified. Herein, the efficacy of PDE2 inhibition is shown to be dependent on intact NO/GC-1/cGMP signaling, as is the case for PDE5 inhibitors (77) [although this esterase may be retargeted in pathological circumstances (78)]. As a consequence, increasing cellular cGMP levels by pharmacological blockade of either PDE2 or PDE5 would be predicted to activate the alternate isozyme as a result of cGMP binding to N-terminal GAF domains possessed by both enzymes (24). This may well explain, at least in part, the lack of efficacy of sildenafil in the RELAX trial, and more positive data in patients would be achieved by dual inhibition of PDE2 and PDE5. However, if both of these PDEs are largely constrained to metabolizing NO/GC-1–derived cGMP, then might combined blockade of PDE2 and PDE9 [which regulates the natriuretic peptide-driven increase in myocardial cGMP (28)] be superior by promoting NO and natriuretic peptide signaling concomitantly? The caveat here is systemic hypotension as a potentially dose-limiting effect when combining cGMP-elevating agents [and other emerging consequences, such as melanoma (79)], so titrating interventions to avoid these concerns would be necessary.

In sum, this study provides convincing evidence in vitro and in vivo of the therapeutic potential of PDE2 inhibition in LVH and HF in promoting cardioprotective cGMP signaling. The beneficial effect of PDE2i is dependent on endogenous NO bioactivity and stimulation of GC-1. Thus, PDE2 inhibition, possibly in combination with other cGMP-elevating agents (e.g., PDE5 and/or PDE9 inhibitors) offers an approach for the treatment of LVH and HF.

ACKNOWLEDGMENTS. This study was supported by British Heart Foundation Grant PG/10/077/28554.

1. Levy D, Garrison RJ, Savage DD, Kannel WB, Castelli WP (1990) Prognostic implications of echocardiographically determined left ventricular mass in the Framingham Heart Study. *N Engl J Med* 322:1561–1566.
2. Abraham WT, Greenberg BH, Yancy CW (2008) Pharmacologic therapies across the continuum of left ventricular dysfunction. *Am J Cardiol* 102:21G–28G.
3. Alexander SP, et al.; CGTP Collaborators (2015) The concise guide to PHARMACOLOGY 2015/16: Enzymes. *Br J Pharmacol* 172:6024–6109.
4. Alexander SP, et al.; CGTP Collaborators (2015) The concise guide to PHARMACOLOGY 2015/16: Overview. *Br J Pharmacol* 172:5729–5743.
5. Calderone A, Thaik CM, Takahashi N, Chang DL, Colucci WS (1998) Nitric oxide, atrial natriuretic peptide, and cyclic GMP inhibit the growth-promoting effects of norepinephrine in cardiac myocytes and fibroblasts. *J Clin Invest* 101:812–818.
6. Zhang YH, Casadei B (2012) Sub-cellular targeting of constitutive NOS in health and disease. *J Mol Cell Cardiol* 52:341–350.
7. Li D, Paterson DJ (2016) Cyclic nucleotide regulation of cardiac sympatho-vagal responsiveness. *J Physiol* 594:3993–4008.
8. Tsai EJ, et al. (2012) Pressure-overload-induced subcellular relocalization/oxidation of soluble guanylyl cyclase in the heart modulates enzyme stimulation. *Circ Res* 110: 295–303.
9. Takimoto E, Kass DA (2007) Role of oxidative stress in cardiac hypertrophy and remodeling. *Hypertension* 49:241–248.
10. Takimoto E, et al. (2005) Oxidant stress from nitric oxide synthase-3 uncoupling stimulates cardiac pathologic remodeling from chronic pressure load. *J Clin Invest* 115:1221–1231.
11. Nakagami H, Takemoto M, Liao JK (2003) NADPH oxidase-derived superoxide anion mediates angiotensin II-induced cardiac hypertrophy. *J Mol Cell Cardiol* 35:851–859.
12. John SW, et al. (1995) Genetic decreases in atrial natriuretic peptide and salt-sensitive hypertension. *Science* 267:679–681.
13. Tamura N, et al. (2000) Cardiac fibrosis in mice lacking brain natriuretic peptide. *Proc Natl Acad Sci USA* 97:4239–4244.
14. Kuhn M, et al. (2002) Progressive cardiac hypertrophy and dysfunction in atrial natriuretic peptide receptor (GC-A) deficient mice. *Heart* 87:368–374.
15. Gheorghiade M, et al.; SOCRATES-REDUCED Investigators and Coordinators (2015) Effect of vericiguat, a soluble guanylate cyclase stimulator, on natriuretic peptide levels in patients with worsening chronic heart failure and reduced ejection fraction: The SOCRATES-REDUCED randomized trial. *JAMA* 314:2251–2262.
16. Ritchie RH, et al. (2009) Exploiting cGMP-based therapies for the prevention of left ventricular hypertrophy: NO* and beyond. *Pharmacol Ther* 124:279–300.
17. Sabine B, et al. (1995) Cyclic GMP-mediated phospholamban phosphorylation in intact cardiomyocytes. *Biochem Biophys Res Commun* 214:75–80.
18. Yang L, et al. (2007) Protein kinase G phosphorylates Cav1.2 alpha1c and beta2 subunits. *Circ Res* 101:465–474.

19. Fiedler B, et al. (2002) Inhibition of calcineurin-NFAT hypertrophy signaling by cGMP-dependent protein kinase type I in cardiac myocytes. *Proc Natl Acad Sci USA* 99: 11363–11368.
20. Tokudome T, et al. (2008) Regulator of G-protein signaling subtype 4 mediates antihypertrophic effect of locally secreted natriuretic peptides in the heart. *Circulation* 117:2329–2339.
21. Koitabashi N, et al. (2010) Cyclic GMP/PKG-dependent inhibition of TRPC6 channel activity and expression negatively regulates cardiomyocyte NFAT activation Novel mechanism of cardiac stress modulation by PDE5 inhibition. *J Mol Cell Cardiol* 48: 713–724.
22. Thoonen R, et al. (2015) Molecular screen identifies cardiac myosin-binding protein-C as a protein kinase G-Iα substrate. *Circ Heart Fail* 8:1115–1122.
23. McMurray JJ, et al.; PARADIGM-HF Investigators and Committees (2014) Angiotensin-neprilysin inhibition versus enalapril in heart failure. *N Engl J Med* 371:993–1004.
24. Bender AT, Beavo JA (2006) Cyclic nucleotide phosphodiesterases: Molecular regulation to clinical use. *Pharmacol Rev* 58:488–520.
25. Miller CL, et al. (2009) Role of Ca2+/calmodulin-stimulated cyclic nucleotide phosphodiesterase 1 in mediating cardiomyocyte hypertrophy. *Circ Res* 105:956–964.
26. Castro LR, Verde I, Cooper DM, Fischmeister R (2006) Cyclic guanosine monophosphate compartmentation in rat cardiac myocytes. *Circulation* 113:2221–2228.
27. Takimoto E, et al. (2005) Chronic inhibition of cyclic GMP phosphodiesterase 5A prevents and reverses cardiac hypertrophy. *Nat Med* 11:214–222.
28. Lee DI, et al. (2015) Phosphodiesterase 9A controls nitric-oxide-independent cGMP and hypertrophic heart disease. *Nature* 519:472–476.
29. Vandeput F, et al. (2009) cGMP-hydrolytic activity and its inhibition by sildenafil in normal and failing human and mouse myocardium. *J Pharmacol Exp Ther* 330: 884–891.
30. Pokreisz P, et al. (2009) Ventricular phosphodiesterase-5 expression is increased in patients with advanced heart failure and contributes to adverse ventricular remodeling after myocardial infarction in mice. *Circulation* 119:408–416.
31. Nagendran J, et al. (2007) Phosphodiesterase type 5 is highly expressed in the hypertrophied human right ventricle, and acute inhibition of phosphodiesterase type 5 improves contractility. *Circulation* 116:238–248.
32. Kim GE, Kass DA (2017) Cardiac phosphodiesterases and their modulation for treating heart disease. *Handb Exp Pharmacol* 243:249–269.
33. Chapman TH, Wilde M, Sheth A, Madden BP (2009) Sildenafil therapy in secondary pulmonary hypertension: Is there benefit in prolonged use? *Vascul Pharmacol* 51: 90–95.
34. Lewis GD, et al. (2007) Sildenafil improves exercise capacity and quality of life in patients with systolic heart failure and secondary pulmonary hypertension. *Circulation* 116: 1555–1562.
35. Guazzi M, Samaja M, Arena R, Vicenzi M, Guazzi MD (2007) Long-term use of sildenafil in the therapeutic management of heart failure. *J Am Coll Cardiol* 50:2136–2144.
36. Guazzi M, Vicenzi M, Arena R, Guazzi MD (2011) PDE5-inhibition with sildenafil improves left ventricular diastolic function, cardiac geometry and clinical status in patients with stable systolic heart failure: Results of a 1-year prospective, randomized, placebo-controlled study. *Circ Heart Fail* 4:8–17.
37. Redfield MM, et al.; RELAX Trial (2013) Effect of phosphodiesterase-5 inhibition on exercise capacity and clinical status in heart failure with preserved ejection fraction: A randomized clinical trial. *JAMA* 309:1268–1277.
38. Aravind L, Ponting CP (1997) The GAF domain: An evolutionary link between diverse phototransducing proteins. *Trends Biochem Sci* 22:458–459.
39. Mehel H, et al. (2013) Phosphodiesterase-2 is up-regulated in human failing hearts and blunts β-adrenergic responses in cardiomyocytes. *J Am Coll Cardiol* 62:1596–1606.
40. Mongillo M, et al. (2006) Compartmentalized phosphodiesterase-2 activity blunts beta-adrenergic cardiac inotropy via an NO/cGMP-dependent pathway. *Circ Res* 98: 226–234.
41. Stangherlin A, et al. (2011) cGMP signals modulate cAMP levels in a compartment-specific manner to regulate catecholamine-dependent signaling in cardiac myocytes. *Circ Res* 108:929–939.
42. Fischmeister R, Hartzell HC (1991) Cyclic AMP phosphodiesterases and Ca2+ current regulation in cardiac cells. *Life Sci* 48:2365–2376.
43. Vettel C, et al. (2017) Phosphodiesterase 2 protects against catecholamine-induced arrhythmia and preserves contractile function after myocardial infarction. *Circ Res* 120:120–132.
44. Zoccarato A, et al. (2015) Cardiac hypertrophy is inhibited by a local pool of cAMP regulated by phosphodiesterase 2. *Circ Res* 117:707–719.
45. Packer M, et al.; The PROMISE Study Research Group (1991) Effect of oral milrinone on mortality in severe chronic heart failure. *N Engl J Med* 325:1468–1475.
46. Bubb KJ, et al. (2014) Inhibition of phosphodiesterase 2 augments cGMP and cAMP signaling to ameliorate pulmonary hypertension. *Circulation* 130:496–507.
47. Baliga RS, et al. (2014) Intrinsic defence capacity and therapeutic potential of natriuretic peptides in pulmonary hypertension associated with lung fibrosis. *Br J Pharmacol* 171:3463–3475.
48. Belteki G, Gertsenstein M, Ow DW, Nagy A (2003) Site-specific cassette exchange and germline transmission with mouse ES cells expressing phiC31 integrase. *Nat Biotechnol* 21:321–324.
49. Moyes AJ, et al. (2014) Endothelial C-type natriuretic peptide maintains vascular homeostasis. *J Clin Invest* 124:4039–4051.
50. Ruetten H, Dimmeler S, Gehring D, Ihling C, Zeiher AM (2005) Concentric left ventricular remodeling in endothelial nitric oxide synthase knockout mice by chronic pressure overload. *Cardiovasc Res* 66:444–453.
51. El-Armouche A, Eschenhagen T (2009) Beta-adrenergic stimulation and myocardial function in the failing heart. *Heart Fail Rev* 14:225–241.
52. Boess FG, et al. (2004) Inhibition of phosphodiesterase 2 increases neuronal cGMP, synaptic plasticity and memory performance. *Neuropharmacology* 47:1081–1092.
53. Hobbs A, Foster P, Prescott C, Scotland R, Ahluwalia A (2004) Natriuretic peptide receptor-C regulates coronary blood flow and prevents myocardial ischemia/reperfusion injury: Novel cardioprotective role for endothelium-derived C-type natriuretic peptide. *Circulation* 110:1231–1235.
54. Lakics V, Karran EH, Boess FG (2010) Quantitative comparison of phosphodiesterase mRNA distribution in human brain and peripheral tissues. *Neuropharmacology* 59: 367–374.
55. Wang L, et al. (2007) Neuronal nitric oxide synthase gene transfer decreases [Ca2+]i in cardiac sympathetic neurons. *J Mol Cell Cardiol* 43:717–725.
56. Liu K, et al. (2018) Phosphodiesterase 2A as a therapeutic target to restore cardiac neurotransmission during sympathetic hyperactivity. *JCI Insight* 3:98694.
57. Mergia E, Friebe A, Dangel O, Russwurm M, Koesling D (2006) Spare guanylyl cyclase NO receptors ensure high NO sensitivity in the vascular system. *J Clin Invest* 116: 1731–1737.
58. Buys ES, et al. (2008) Gender-specific hypertension and responsiveness to nitric oxide in sGCalpha1 knockout mice. *Cardiovasc Res* 79:179–186.
59. Xie M, Burchfield JS, Hill JA (2013) Pathological ventricular remodeling: Therapies: Part 2 of 2. *Circulation* 128:1021–1030.
60. Mokni W, et al. (2010) Concerted regulation of cGMP and cAMP phosphodiesterases in early cardiac hypertrophy induced by angiotensin II. *PLoS One* 5:e14227.
61. Moltzau LR, et al. (2014) Differential regulation of C-type natriuretic peptide-induced cGMP and functional responses by PDE2 and PDE3 in failing myocardium. *Naunyn Schmiedebergs Arch Pharmacol* 387:407–417.
62. Tsai EJ, Kass DA (2009) Cyclic GMP signaling in cardiovascular pathophysiology and therapeutics. *Pharmacol Ther* 122:216–238.
63. Kuhn M (2016) Molecular physiology of membrane guanylyl cyclase receptors. *Physiol Rev* 96:751–804.
64. Balashova N, Chang FJ, Lamothe M, Sun Q, Beuve A (2005) Characterization of a novel type of endogenous activator of soluble guanylyl cyclase. *J Biol Chem* 280:2186–2196.
65. Antonova G, et al. (2007) Functional significance of hsp90 complexes with NOS and sGC in endothelial cells. *Clin Hemorheol Microcirc* 37:19–35.
66. Bendall JK, et al. (2004) Role of myocardial neuronal nitric oxide synthase-derived nitric oxide in beta-adrenergic hyporesponsiveness after myocardial infarction-induced heart failure in rat. *Circulation* 110:2368–2375.
67. Liu Y, et al. (2013) Volume overload induces differential spatiotemporal regulation of myocardial soluble guanylyl cyclase in eccentric hypertrophy and heart failure. *J Mol Cell Cardiol* 60:72–83.
68. Bubikat A, et al. (2005) Local atrial natriuretic peptide signaling prevents hypertensive cardiac hypertrophy in endothelial nitric-oxide synthase-deficient mice. *J Biol Chem* 280:21594–21599.
69. Lukowski R, et al. (2010) Cardiac hypertrophy is not amplified by deletion of cGMP-dependent protein kinase I in cardiomyocytes. *Proc Natl Acad Sci USA* 107:5646–5651.
70. Buys ES, et al. (2007) Cardiomyocyte-restricted restoration of nitric oxide synthase 3 attenuates left ventricular remodeling after chronic pressure overload. *Am J Physiol Heart Circ Physiol* 293:H620–H627.
71. Ichinose F, et al. (2004) Pressure overload-induced LV hypertrophy and dysfunction in mice are exacerbated by congenital NOS3 deficiency. *Am J Physiol Heart Circ Physiol* 286:H1070–H1075.
72. Patrucco E, et al. (2014) Roles of cGMP-dependent protein kinase I (cGKI) and PDE5 in the regulation of Ang II-induced cardiac hypertrophy and fibrosis. *Proc Natl Acad Sci USA* 111:12925–12929.
73. Blanton RM, et al. (2012) Protein kinase g iα inhibits pressure overload-induced cardiac remodeling and is required for the cardioprotective effect of sildenafil in vivo. *J Am Heart Assoc* 1:e003731.
74. Frantz S, et al. (2013) Stress-dependent dilated cardiomyopathy in mice with cardiomyocyte-restricted inactivation of cyclic GMP-dependent protein kinase I. *Eur Heart J* 34:1233–1244.
75. Spiessberger B, et al. (2009) cGMP-dependent protein kinase II and aldosterone secretion. *FEBS J* 276:1007–1013.
76. Meier S, et al. (2017) PDE3 inhibition by C-type natriuretic peptide-induced cGMP enhances cAMP-mediated signaling in both non-failing and failing hearts. *Eur J Pharmacol* 812:174–183.
77. Takimoto E, et al. (2005) cGMP catabolism by phosphodiesterase 5A regulates cardiac adrenergic stimulation by NOS3-dependent mechanism. *Circ Res* 96:100–109.
78. Zhang M, et al. (2012) Pathological cardiac hypertrophy alters intracellular targeting of phosphodiesterase type 5 from nitric oxide synthase-3 to natriuretic peptide signaling. *Circulation* 126:942–951.
79. Dhayade S, et al. (2016) Sildenafil potentiates a cGMP-dependent pathway to promote melanoma growth. *Cell Rep* 14:2599–2610.